A Comparison of Four Methods for Determining Precipitable Water Vapor Content from Multi-Spectral Data

Karen Lewis Hirsch, Lee Balick, Christoph Borel, and
Peter McLachlan

Los Alamos National Laboratory,
Space and Remote Sensing Science Group (NIS-2)
P.O. Box 1663 Mail Stop C-323, Los Alamos, NM 87545

ABSTRACT

Determining columnar water vapor is a fundamental problem in remote sensing. This measurement is important both for understanding atmospheric variability and also from removing atmospheric affects from remotely sensed data. Therefore, discovering a reliable, and if possible, automated method for determining water vapor column abundance is important. There are two standard methods for determining precipitable water vapor during the daytime from multi–spectral data. The first method is the Continuum Interpolated Band Ratio (CIBR) (see for example King, et al., 1996[1]). This method assumes a baseline and measures the depth of a water vapor feature as compared to this baseline. The second method is the Atmospheric Pre–corrected Differential Absorption technique (APDA) (see Schläpfer, et al., 1998[2]); this method accounts for the path radiance contribution to the top of atmosphere radiance measurement, which is increasingly important at lower and lower reflectance values. We have also developed two methods of modifying CIBR. We use a simple curve fitting procedure to account for and remove any systematic errors due to low reflectance while still preserving the random spread of the CIBR values as a function of surface reflectance. We also have developed a two–dimensional look-up table for CIBR; CIBR, using this technique, is a function of both water vapor (as with all CIBR techniques) and surface reflectance. Here we use data recently acquired with the Multi–spectral Thermal Imager spacecraft (MTI) to compare these four methods of determining columnar water vapor content.

Keywords: MTI, Multispectral Imaging, Water Vapor Algorithms

1. INTRODUCTION

Atmospheric absorption can lead to misinterpretation of surface features and temperatures. This misinterpretation can come about because one is looking for a mineral or other substance that has a feature within an atmospheric feature; for example iron has a feature near a water vapor line in the near infrared (around 940 nm). In the thermal infrared the atmosphere can modify the apparent temperature within a pixel. Removing the atmospheric effects can lead to more appropriate temperature retrievals.

The Multispectral Thermal Imager (MTI) was launched in the spring of 2000. This spacecraft has a core mission of quantitatively testing and demonstrating certain aspects of remote sensing. Specifically, one of the goals requires determination of accurate ground temperatures. Since the presence of water vapor can effect the ground temperature determination from spacecraft imagery, we are interested in developing reliable methods for determining water vapor column abundances for later atmospheric correction.

Figure 1 shows the relative positions of the MTI spectral bands E, F and G. These bands were chosen to allow easy water vapor calculations to be made (see Clodius et al., 1998[3] for a further description of MTI spectral band selections.) We will hence-force use band F to describe the 940 nm water vapor absorption feature and bands E and G to refer to the reference bands around the 940 nm absorption feature.

Beyond the MTI interest, many others have an interest in determining accurate water vapor column abundance measurements (WV) from imagery. For atmospheric physicists and climatologists, water vapor is an important physical quantity to be surveyed and studied. Since atmospheric WV is both a greenhouse gas in its own right and a proxy for other greenhouse gases its variability over time and space are often studied by climatologists.

Further author information: (Send correspondence to K.L.H.)
K.L.H.: E-mail: hirsch@lanl.gov; Telephone: (505) 667-9006; Fax: (505) 667-9208
L.B.: E-mail: lbalick@lanl.gov
C.B.: E-mail: cborel@lanl.gov
P.M.: E-mail: pmclachlan@lanl.gov
W.C.: E-mail: wclodius@lanl.gov

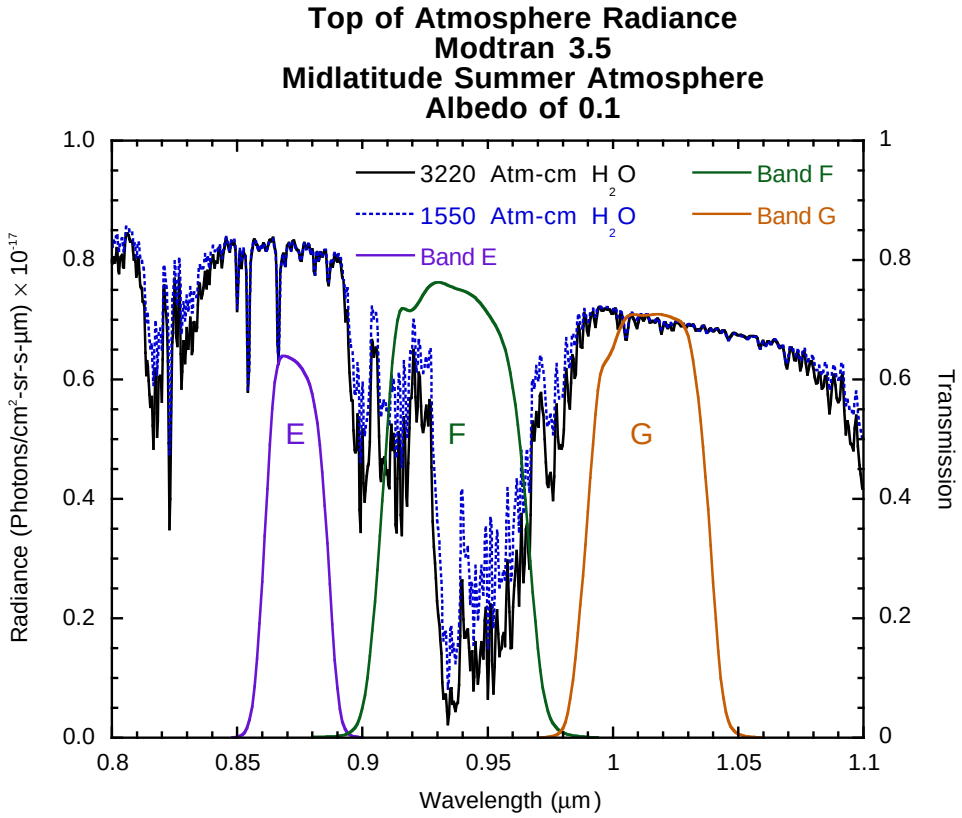

Figure 1. The MTI spectral bands E, F, and G and the radiance spectrum around the water vapor spectral feature at 940nm

Some studies pursued using WV are related to large scale atmospheric variability,[4] while others might pursue small scale turbulence (∼50m) and eddies (see for example Kao, et al.[5]).

The two leading methods for determining water vapor column abundance (WV) are the Continuum Interpolated Band Ratio (CIBR)[1] and the Atmospheric Pre-corrected Differential Absorption (APDA).[2] CIBR is a simple band ratio method for determining water vapor abundance. Due to its simplicity, it is least effective over dark targets (like water). APDA is a slightly more complex band ratio method. Here the path radiance is subtracted from the total radiances before the ratio is computed, thus accounting for path radiance contributions. Both of these initial methods are described in the preceding paper.[6] We also created two modified versions of CIBR. First we used a simple curve fitting procedure outlined in Balick et al., 2000.[7] The other modified version of CIBR uses the surface reflectances as one of the inputs.

2. CIBR

CIBR is a simple band ratio:

$$CIBR = \frac{F}{w_1 E + w_2 G} \tag{1}$$

where E, F, and G represent the radiance values in these MTI bands. Band F has its band center in the 940nm water vapor feature, while E and G have their band centers outside this feature. w_1 and w_2 are relative weighting factors for how far between E and G band F's center resides. This ratio is then used to interpolate a look-up table of CIBR as a function of WV. This look-up table is created using MODTRAN 4 with the correct target location, spacecraft location, sun and view angles, and time of image.

This general method has been used with AVIRIS, ATSR, MODIS[8,9] and other hyper-spectral and multispectral sensors (see for example Tahl and von Schonermark[10]). This is a very simple and quick method. It works best over bright targets, like forest. It works not as well over dark targets, like water.

3. APDA

APDA is an augmented CIBR.[2] This method corrects for path radiance in the absorption band by using MODTRAN4 determined path radiance as a function of water vapor column abundance. Thus the method can be described by iterating between a set of coupled equations, one based on data and the other on MODTRAN:

$$APDA_{data} = \frac{F_{data} - Path_F(WV)}{w_1(E_{data} - Path_E) + w_2(G_{data} - Path_G)} \quad (2)$$

$Path_F(WV)$ is a second order polynomial fit to the values of $Path_F$ as a function of WV calculated from MODTRAN 4. $Path_E$ and $Path_G$ are water vapor independent, due to their position outside the water vapor feature at 940nm. A similar relationship is derived for $APDA_{model}$ using band averaged radiance values derived from MODTRAN 4 run at a surface reflectance of 0.45 as a function of WV. This $APDA_{model}$(WV) is then interpolated so that a WV value is returned for each value of $APDA_{data}$. This is described in much more detail in the preceding paper.[6]

The automated version of APDA implemented is not optimal. While it is possible for APDA to do much better than CIBR over dark pixels (like water), this requires a good knowledge of the aerosols and the visibility. When these quantities are tweaked, APDA does not usually show more than a pixel or two boundary at water (due perhaps to registration issues), and otherwise the water appears to have the same amount of WV as the land (approximately, and using lake scenes).

4. Modified CIBR - Curve Fit

We know that CIBR has trouble over dark targets, due to its failure to correct for path radiance. Here we fit two curves to the relationship between CIBR and TOA reflectance. A linear regression is fit to CIBR for all values of reflectance greater than 0.2. A second curve is fit to all data with a second order polynomial fit to the log of CIBR. The difference between the curves is added - resulting in a modified CIBR which essentially removes some systematic dependence on CIBR at low reflectance while preserving the random spread of the values around a mean CIBR value.[7] Figure 2 illustrates before and after CIBR versus surface reflectance has been modified for the AVIRIS image of BOREAS - in an MTI-like form (re-sampled to the MTI spectral channels).[7]

5. Modified CIBR - Look-up table function of surface reflectance

As noted in the previous section, the major trouble with CIBR is its unreliability over dark targets. Presumably, part of this is due to a failure to account for the changes in surface reflectance. Thus, we investigated using multiple look-up tables to transition between CIBR and WV - each at a different value of surface reflectance. We then nearest neighbor sampled for each point in the image, so that it used the closest appropriate look-up table. The six values of surface reflectances used for the look-up table are weighted toward low values: 0.0, 0.05, 0.1, 0.2, 0.4, and the maximum value in the image were used for this study.

Note that we find that running MODTRAN is quite time consuming. Consequently, this method - requiring multiple look-up tables takes the longest time to run (by a factor of almost 6 on a standard Linux box with dual Pentium three processors running at 500 MHz). Clearly, though, this method could be run in parallel in future efforts, and sped up through that process.

6. Validation: CIBR and APDA

Here we demonstrate that our original APDA and CIBR implementations return reasonable values. We have used data from the following sources to aid in validating both unmodified water vapor algorithms: Savannah River Technology Center radiosonde, Savannah River Technology Center sun photometer, Jet Propulsion Laboratory radiosonde, the radiosonde data available from the NOAA FSL, the Aeronet set of sun photo-meter data, and the line of site (LOS) data from the Southern Great Plains ARM site.

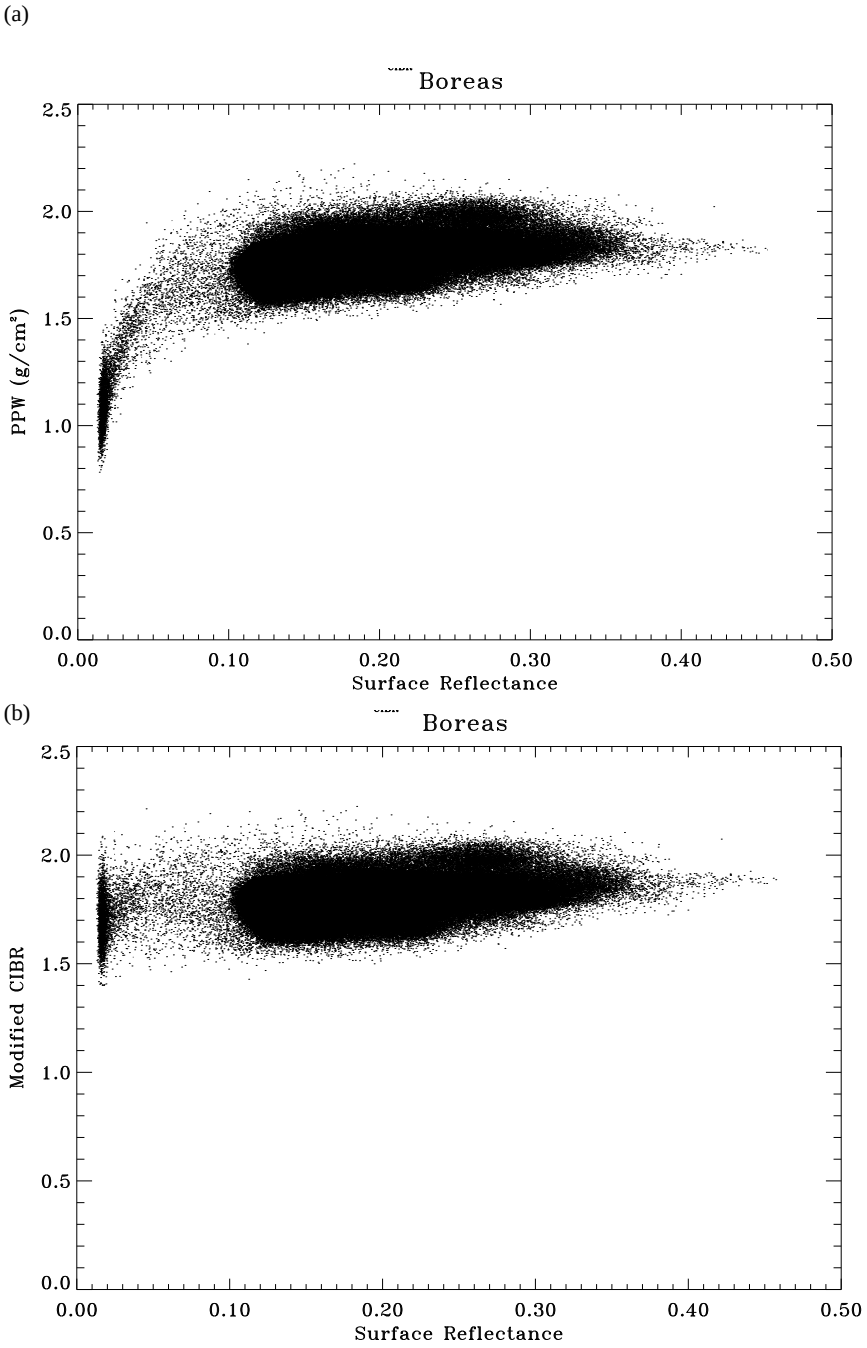

Figure 2. (a) Unmodified relationship between CIBR and reflectance and (b) modified relationship between CIBR and reflectance for BOREAS

Table 1: Ground and In Situ Data as compared to APDA and CIBR Retrievals in $\frac{g}{cm^2}$, ** indicates APDA failure to converge to positive real value. Aeronet sun photometer at Mauna Loa is slightly lower in altitude than the Mauna Loa location we used for comparison

Site	Date	Image ID	APDA	CIBR	Validation Data	Source
Ivanpah	09/15/00	29243	1.30	1.24	1.35	SRTC balloon
Ivanpah	09/15/00	29243	1.30	1.24	1.24	sun photometer
Ivanpah	09/15/00	29250	1.23	1.18	1.35	SRTC balloon
Ivanpah	09/15/00	29250	1.23	1.18	1.24	sun photometer
Ivanpah	09/16/00	29316	1.25	1.20	1.24	sun photometer
Ivanpah	09/16/00	29323	1.26	1.19	1.24	sun photometer
Mauna Loa	06/12/00	18498	0.15	0.15	0.32	Aeronet
Mauna Loa	06/12/00	18498	0.15	0.15	0.215	NOAA FSL
Mauna Loa	06/12/00	18505	0.46	0.15	0.32	Aeronet
Mauna Loa	06/12/00	18505	0.46	0.15	0.215	NOAA FSL
Mauna Loa	07/15/00	20926	0.86	0.81	0.82	Aeronet
Mauna Loa	07/15/00	20926	0.86	0.81	0.82	JPL Radiosonde
Mauna Loa	07/15/00	20926	0.86	0.81	0.615	NOAA FSL
Mauna Loa	07/15/00	20933	**	0.60	0.82	Aeronet
Mauna Loa	07/15/00	20933	**	0.60	0.82	JPL Radiosonde
Mauna Loa	07/15/00	20933	**	0.60	0.615	NOAA FSL
Mauna Loa	10/09/00	31823	0.10	0.11	0.133	NOAA FSL
Mauna Loa	10/09/00	31830	0.35	0.12	0.133	NOAA FSL
Nauru	05/19/00	17045	3.68	3.53	5.5	Aeronet
Nauru	07/02/00	20096	**	3.11	3.7	JPL Radiosonde
Nauru	07/03/00	19774	3.43	3.30	4.2	Aeronet
Nauru	07/03/00	19781	2.42	3.73	4.2	Aeronet
Nauru	08/05/00	22793	4.46	4.32	5.9	Aeronet
Nauru	08/05/00	22800	**	4.26	5.9	Aeronet
Point Barrow	10/12/00	32496	**	0.70	0.912	NOAA FSL
Point Barrow	10/12/00	32503	0.41	0.70	0.912	NOAA FSL
Stennis	06/02/00	17819	2.94	2.89	3.6	Aeronet
Stennis	06/02/00	17826	3.52	3.52	3.6	Aeronet
Stennis	07/29/00	22193	3.54	3.47	4.5	Aeronet
Stennis	07/29/00	22200	3.50	3.74	4.5	Aeronet
Stennis	08/10/00	23277	3.75	4.13	6.2	Aeronet
Stennis	08/10/00	23284	**	4.27	6.2	Aeronet
Stennis	08/21/00	26240	3.73	3.90	5.2	Aeronet
Stennis	08/21/00	26247	**	4.10	5.2	Aeronet
SGP ARM	08/24/00	26556	3.06	2.93	3.57	ARM LOS
SGP ARM	08/24/00	26563	3.35	3.15	3.59	ARM LOS
SGP ARM	08/25/00	26648	2.70	2.60	3.00	ARM LOS
SGP ARM	08/25/00	26655	2.77	2.60	3.03	ARM LOS
SGP ARM	08/26/00	26747	2.90	2.75	3.16	ARM LOS
SGP ARM	08/26/00	26754	3.01	2.92	3.32	ARM LOS

As the water vapor validation values increase, the CIBR and APDA values diverge further - see Figure 3. For values of water vapor validation data over 3.5, we find the divergence between CIBR and APDA derived data and the validation data to be greater.

7. Side by Side Comparison

We compare all four methods with three very different images. The first image is of Crater Lake. High in the mountains, it should have very low values for water vapor, and a very deep lake - which poses problems both to APDA and to CIBR - see Figure 4. For APDA (a) we find that the lake has a much lower WV value. This is due to having the visibility set to 23 km. When tropospheric aerosols (50 km visibility) is used, the lake comes out

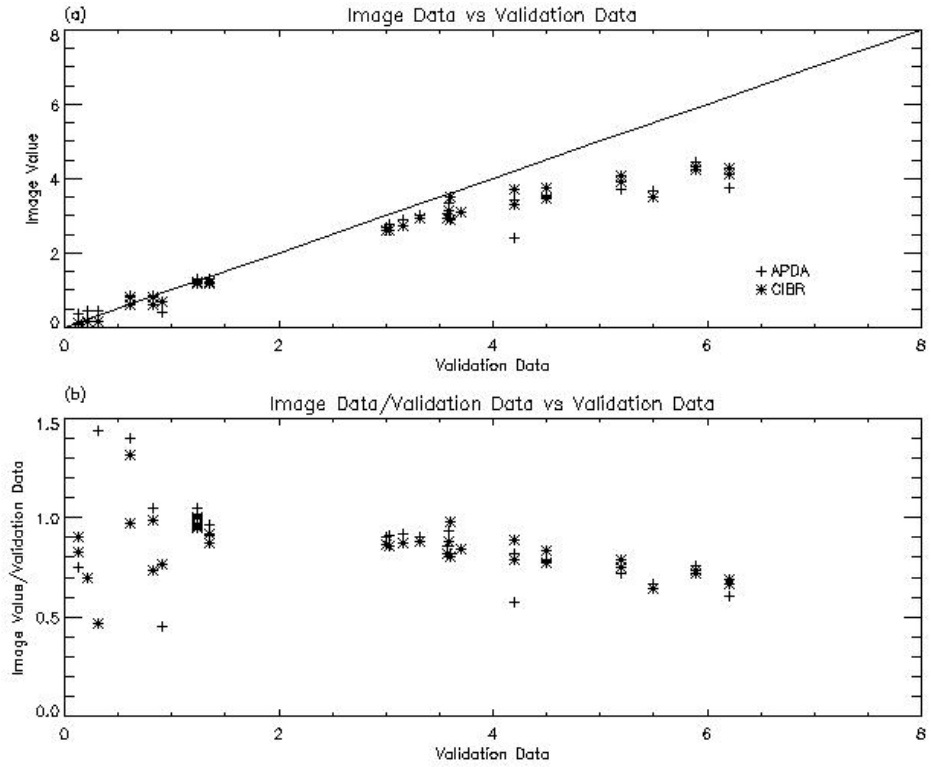

Figure 3. (a) Image data versus validation data. Asterisks are CIBR values, plus signs are APDA values. (b) Image data/validation data compared to validation data.

with a higher value). For unmodified CIBR (b) we find that the lake is doing better than APDA, but still not great. Using the fit CIBR (c) does much better over the lake, but it is not clear that the values are quite that high in the lake. Rho dependent CIBR (d) does as well as the fit CIBR - except at the edges of the lake.

The next comparison was at Nauru. Part of the TWP-ARM site, we have validation data for the Nauru image in question. One of the questions was how well the modified CIBR curve fitting would work in the presence of clouds. Since clouds do not occur at a specific reflectance, the empirical curve fitting was using cloud data in its curve fitting routines (along with ground data). The results can be seen in Figure 5. In (a) APDA derived the water has too low a WV value over water. In (b) the CIBR has too low a WV value over water - but it is a significant improvement over the APDA values (when the aerosol model is not matched perfectly). In (c) there is a little flakiness due to the clouds (especially on the left edge of the image) and due to the fact that the fitting procedure fit each panel within the image - rather than the image as a whole. Since there is no land on the left edge the whole WV value for that edge is effected only by the clouds. Finally in (d) we see that the whole image is smoothly fit. The water vapor values for the image are much higher in this image as well - 3.93 as opposed to the values of 3.3 (or so) for the unmodified CIBR. The truth for this image was 4.1, so the fit as a function of surface reflection offers the greatest match to the 'truth.'

Finally, we examined an SGP-ARM image in Figure 6. What stands out in this image is that the edges of farm fields are visible in the unmodified CIBR image. While the edges of the fields is not erased - and this might be due to very slight (sub-pixel) mis-registration within the image, relative differences in water vapor between the fields are lessened in the APDA and both modified CIBR images. Thus any of the modified CIBR images is an improvement in this case. In this case, the APDA in (a) shows some beautiful structure. The fields and other topographic details are not seen. The CIBR image (b) shows each individual field. This is not physical - and therefore a significantly poorer result than the APDA result. The fit CIBR (c) again shows fields - especially on the left edge of the image. It is not an improvement over the unmodified CIBR. Finally, the rho dependent CIBR (d) image shows much less of the field structure. Here the structure apparent in APDA shows up - but to a much smaller extent.

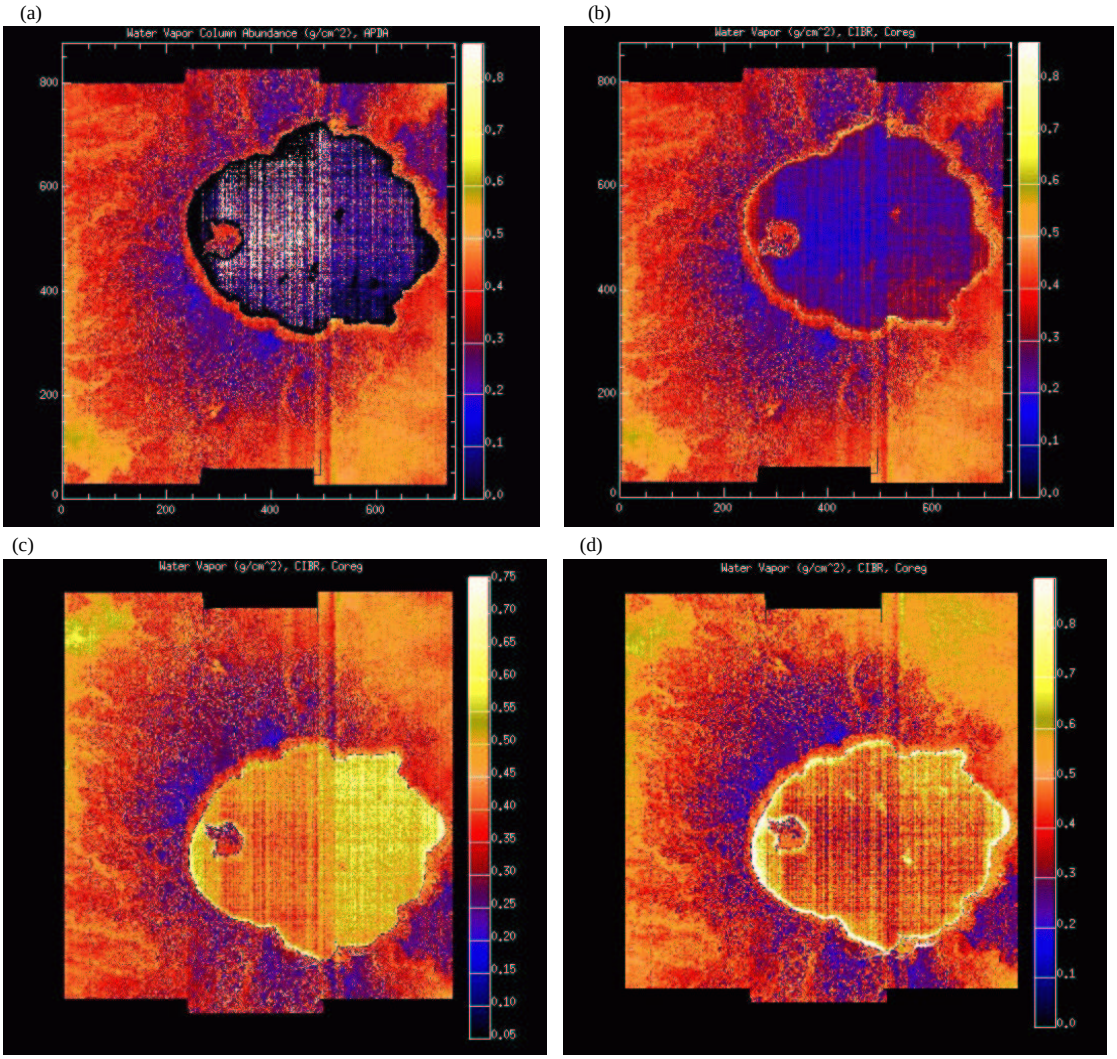

Figure 4. (a) APDA for Crater Lake. (b) CIBR unmodified. (c) CIBR with curve fit. (d) CIBR as a function of surface reflectance

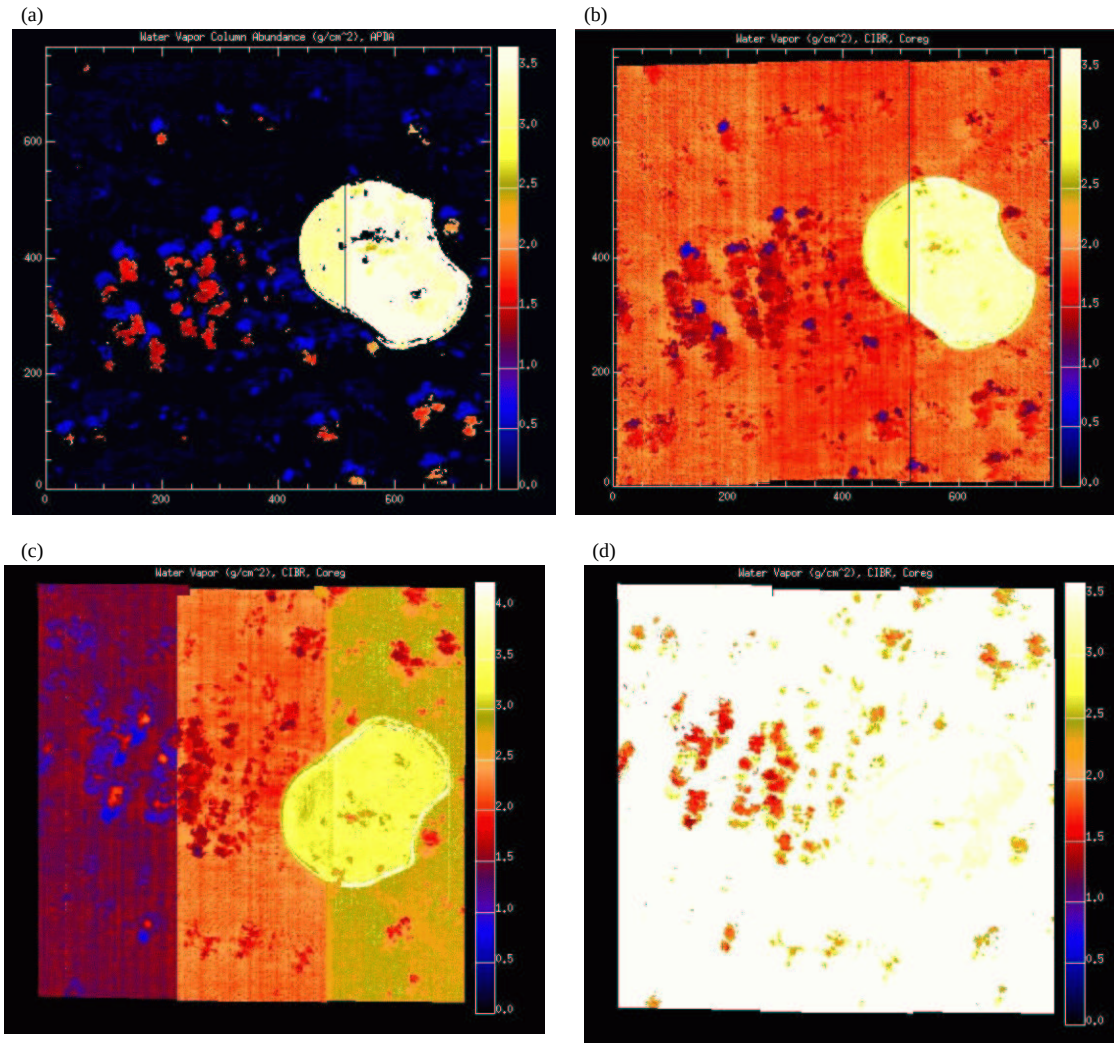

Figure 5. (a) APDA for Nauru. Note that failure to match the aerosol precisely leads to very low values over water. (b) CIBR unmodified. Island still has higher WV values than the water. (c) CIBR with curve fit. (d) CIBR as a function of surface reflectance

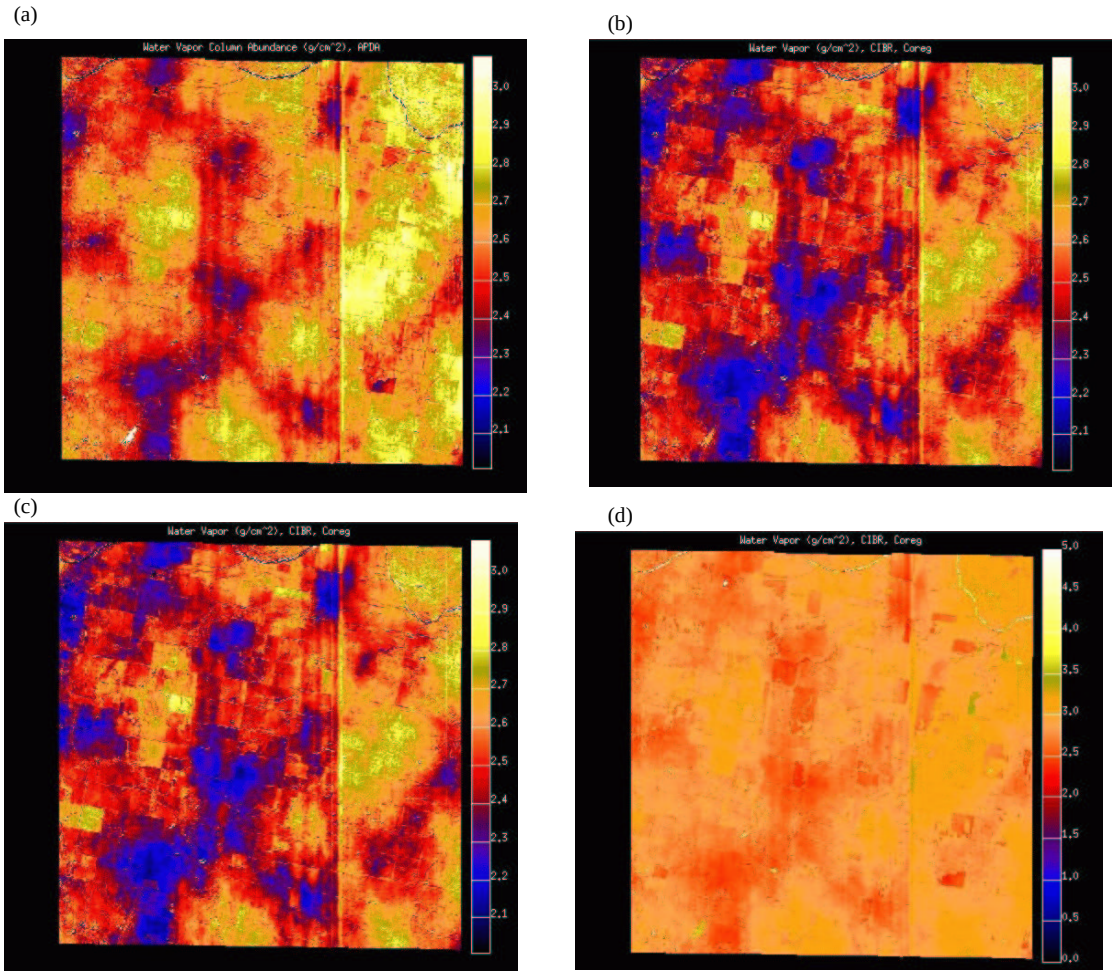

Figure 6. (a) APDA for SGP-ARM. (b) CIBR unmodified. (c) CIBR with curve fit. (d) CIBR as a function of surface reflectance

8. Conclusions

Four methods for determining water vapor column abundances have been compared. These are a version of CIBR, a version of APDA, a fit CIBR and CIBR as a function of surface reflectance. Each method has certain limitations.

CIBR is a quicker and simpler method than APDA. It has been shown to work consistently poorly over dark targets like water. It does reasonably well over more reflective targets, like green vegetation. Our implementation is within 0.5 cm of water from concurrent ground measurements - unless there is more than 4 cm of water in the concurrent ground measurement.

APDA is a better routine, but only when we know the visibility and the aerosol model reasonably well. We expect that when the Aerosol retrieval for MTI is optimized, we will be able to use that to make APDA into a superior method for determining water vapor over darker surfaces. In the meanwhile, there are some outstanding APDA issues. APDA, in very wet scenes, sometimes fails to converge to physical values (positive WV) in off-nadir images. APDA is not a significant improvement over CIBR as long as the aerosols are not modeled correctly in MODTRAN. APDA is within 0.5 cm of water when compared to concurrent ground measurements unless the ground measurement has more than 4 cm of water.

Both of these methods can be trusted to do a first cut at determining which images are wet. They can also be used in optimizing water temperature retrievals, though they both work best when some land is in the image.

The empirical fitting of CIBR as a function of surface reflectance works best in cloud–free and snow/ice–free images. In images where there is not land in each of the sub-images, the current implementation fails. In short, using the unmodified CIBR is preferable to this modified version.

The CIBR as a function of both surface reflectance and WV appears to be the best routine in terms of results, but the most computationally intensive. It does not have problems with clouds. It seems to do better at determining higher amounts of WV. It does not fail on off-nadir images - as APDA does when the aerosols are not perfectly matched. No land is required in the image for it to work well.

9. Future Work

Implementing a fitting routine that is for the whole image, rather than the sub-image (SCA specific) as it is now implemented will improve the fit results. Unfortunately, as long as their are clouds, this may not be the optimal method.

Parallelizing the multiple look-up tables might make it feasible to use the CIBR as a function of both surface reflectance and WV.

Finally, quantifying the difference between APDA and the CIBR as a function of surface reflectance would be very important in deciding which one is better. It would be best to have a daytime over-flight of LIDAR to build a two dimensional validation map for this quantitative assessment.

ACKNOWLEDGMENTS

Work was supported by the U.S. Department of Energy under Contract W-7405-ENG-36.

REFERENCES

1. M. D. King, W. P. Menzel, P. S. Grant, J. S. Myers, G. T. Arnold, S. E. Platnick, L. E. Gumley, S. C. Tsay, C. C. Moeller, M. Fitzgerald, K. S. Brown, and F. G. Osterwisch, "Airborne scanning spectrometer for remote sensing of cloud, aerosol, water vapor and surface properties," *J. Atmos. Oceanic Technol.* **13**, pp. 777–794, 1996.
2. D. Schläpfer, C. C. Borel, J. Keller, and K. I. Itten, "Atmospheric precorrected differential absorption technique to retrieve columnar water vapor," *Remote Sensing of Environment* **65**(3), pp. 353–366, 1998.
3. W. B. Clodius, P. G. Weber, C. C. Borel, and B. W. Smith, "Multi–spectral band selection for satellite–based systems," *Proc. SPIE* **3377**, pp. 11–21, 1998.
4. M. T. Chahine, "The hydrological cycle and its influence on climate," *Nature* **359**, pp. 32141–32158, 1992.
5. C. Y. J. Kao, Y. H. Hang, D. I. Cooper, W. E. Eichinger, W. S. Smith, and J. M. Reisner, "High–resolution modeling of LIDAR data mechanisms governing surface water vapor variability during SALSA," *Agricultural and forest meteorology* **105**, pp. 185–194, 2000.
6. C. Borel, K. L. Hirsch, and L. K. Balick, "Recipes for writing algorithms to retrieve columnar water vapor for 3-band multispectral data," *Proc. SPIE* **4381**, 2001. in press.

7. L. K. Balick, C. C. Borel, K. L. Hirsch, and P. S. McLachlan, "Implementation and validation of atmospheric compensation algorithms for multispectral thermal imager pipeline processing," *Proc. SPIE* **4125**, 2000.
8. B.-C. Gao and Y. J. Kaufman, "Derivation of column atmospheric water vapor amount for MODIS near–IR channels," *IGARSS 2000. IEEE 2000 International Geoscience and Remote Sensing Symposium. Taking the Pulse of the Planet: The Role of Remote Sensing in Managing the Environment* , 2000.
9. B.-C. Gao, Y. Kaufman, and W. Han, "Retrieval of column water vapor amount from MODIS channels near 1μm," *IGARSS 1998. Sensing and Managing the Environment. 1998 IEEE International Geoscience and Remote Sensing Symposium* , 1998.
10. S. Tahl and M. von Schonermark, "Determination of the column water vapour of the atmosphere using backscattered solar radiation measured by the Modular Optoelectronic Scanner (MOS)," *International Journal of Remote Sensing* **19**(17), pp. 3223–36, 1998.